A MISSION ANALYSIS SOFTWARE FOR SMALL SATELLITES

Sahin Ulas Koprucu[1]
University of Turkish Aeronautical Association

Halis Abdullah Ozcelik[2], Sulenur Altunay[3]
Middle East Technical University

Burak Yaglioglu[4]
TUBITAK UZAY
Space Technologies Research Institute
Ankara, Turkey

Ozan Tekinalp[5]
Middle East Technical University
Ankara, Turkey

ABSTRACT

In this paper, a mission analysis software is described for LEO small satellites which is developed by students participating in the APSCO (Asia-Pacific Space Cooperation Organization) Student Small Satellite (SSS) project. The software currently includes several functionalities such as orbit propagation with the options of SGP4 and numerical integration as well as calculation of groundtracks, eclipse durations, solar and albedo fluxes on the satellite panels, communication intervals, imaging opportunities and parameters specific to satellite modes. The results of the most functions are compared and verified with General Mission Analysis Tool (GMAT). For the further analysis, it is considered to include specific attitude profiles, and thermal analysis capabilities. It is aimed that this work would a baseline for a highly capable mission analysis software which can be used by universities and research institution for the design, analysis and operations of LEO small satellites.

INTRODUCTION

The utilization of small satellites has increased substantially over the course of past 15 years. As of June 2019, over 1000 CubeSats have been launched and developers are composed of not only universities and research institutions, but also private companies and government organizations [Kulu,2019]. This is mainly due to the fact that they can perform similar or part of the functionalities of standard satellites, with less cost and easier accessibility.. For instance, Student Small Satellite (SSS) Program of the Asia Pacific Space Cooperation Organization (APSCO) aims to foster research, education and capacity building among the Member States through the utilization of a constellation of 1 Microsat, SSS-1, of around 30 kg

---

[1] Senior Student in Department of Astronautical Engineering, sahinulas.koprucu@hotmail.com
[2] Senior Student in Department of Aerospace Engineering, hlsabdullah27@gmail.com
[3] Senior Student in Department of Aerospace Engineering, sulenuraltunay@gmail.com
[4] Chief Researcher, Attitude and Orbit Control Group, burak.yaglioglu@tubitak.gov.tr
[5] Professor, Department of Aerospace Engineering, tekinalp@metu.edu.tr

and 2 Cubesats with 3U size, SSS-2A and 2B. Here, SSS-2B satellite is led by TUBITAK UZAY (Space Technologies Research Institute of the Scientific and Technological Research Council of Turkey) on behalf of the Turkish Consortium [Yaglıoglu,et. al.,2019]. In the SSS-2B project, faculty members and students from Middle East Technical University (METU) and University of Turkish Aeronautical Association (UTAA) are also incorporated in the design, development and operations of the satellite.

Although the interest in small satellites is high, not all entities are able to evaluate their mission ideas and assess the feasibility. In this manner, there is a need for a mission analysis tool which is responsive to the user's needs and capable of incorporating functionalities for advanced analysis. In addition, mission analysis plays an important role in both design phase and nominal operations of a space mission. Several parameters related to mission, orbit, power generation and thermal control are determined from the mission analysis in the design phase. Also, mission analysis provides information for the operational tasks such as planning of satellite modes and maneuvers as well as the calculation of communication intervals and imaging opportunities.

There are already available mission analysis tools such as STK (Systems Tool Kit) and GMAT (General Mission Analysis Tool) which are highly capable in terms of different analysis and have extensive area of usage. GMAT is an open source software and includes essential tools. On the other hand, STK is a commercial software whose utilization is limited to its built-in functionalities and may not be available for every instittution. Here, GMAT is an open source and available software, however it lacks some of the functionalities such as orbit propagation with SGP4, calculation of solar and albedo fluxes on the satellite panels, imaging opportunities and other parameters related to specific modes of a satellite.

In this paper, a mission analysis software is described for Low Earth Orbit (LEO) small satellites which is developed by students involved within the Turkish Consortium of the APSCO) SSS project. The developed software currently includes several functionalities such as orbit propagation with the options of SGP4 and numerical integration, groundtrack plots as well as calculations of the eclipse durations, solar and albedo fluxes on the satellite panels, communication intervals, imaging opportunities and parameters varying with the satellite modes. The outputs of the most functions are compared and verified with GMAT. For the further analysis, it is considered to include attitude profile for each mode, and thermal analysis capabilities. At the end of this work, a highly capable mission analysis software is aimed which can be used for the design, analysis and operations of LEO small satellites.

SOFTWARE FUNCTIONS

The software currently includes several functions related to LEO missions such as orbit propagation, groundtrack plots as well as calculations of the eclipse durations, solar and albedo fluxes on the satellite panels, communication intervals, imaging opportunities and parameters varying with the satellite modes. In this section, those functions are explained with detail.

Orbit Propagation

The starting point of a mission analysis is the propagation of orbit which is basically the calculation of the trajectory of a satellite. There are mainly two type of propagators: analytical and numerical. Analytical propagators are faster however less accurate and they can be used in short term analysis. On the other hand, numerical propagators are computationally more demanding with high accuracy and, therefore, they can be used in long term analysis. The most well-known analytical propagator is the SGP4 model. It works with Two Line Element (TLE) set which includes information about the orbital elements and reference time. On the other hand, numerical propagators differ with respect to the numerical integration method,

force configurations and assumptions on dynamics . Mostly, the state vector obtained from an orbit determination result is input to the numerical propagators.

In the software, both numerical and analytical propagators are used. For the analytical propagator, SGP4 model is used. For the numerical propagator, the trajectory of the satellite is obtained by numerically integrating the equation of motion

$$\ddot{\vec{r}} = -\frac{\mu}{r^3}\vec{r} + \vec{p}_{J2} + \vec{p}_{Drag}, \tag{1}$$

considering the 2-Body acceleration as well as perturbations due to oblateness of the Earth $\vec{p}_{J2}$ and atmospheric drag $\vec{p}_{Drag}$. Here μ is the gravitational parameter of the Earth and $\vec{r}$ is the position vector of the satellite in Earth Centered Inertial (ECI) frame. Equation (1) is a second order ordinary differential equation and Dormand-Prince [Dormand and Prince, 1980] method is used with fixed stepsize for numerical integration. Two force models are used in the equation of motion: effect of Earth oblateness (J2 perturbation) and atmospheric drag which will be described in the following sub-sections.

Earth Oblateness (J2 Perturbation)

The gravitational field of Earth is not uniform due to non-homogeneous mass distribution. One of the major perturbing acceleration which is due to Earth's oblateness is given as

$$\vec{p}_{J2} = \frac{3}{2}\frac{J_2\mu R^2}{r^4}\left[\frac{x}{r}\left(5\frac{z^2}{r^2}-1\right)\hat{\imath} + \frac{y}{r}\left(5\frac{z^2}{r^2}-1\right)\hat{\jmath} + \frac{z}{r}\left(5\frac{z^2}{r^2}-3\right)\hat{k}\right], \tag{2}$$

where J_2 is the largest zonal harmonic of Earth and it is found experimentally, R is the radius of Earth and x, y, z are the components of the position vector of the satellite in Earth Centered Earth Fixed Frame (ECEF) which is a frame rotating with Earth. Since ECEF is not an inertial frame, the ECI to ECEF transformation is required:

$$\vec{r}_{ECEF} = M(t)ROT3\big(\theta_{GAST}(t)\big)N(t)P(t)\vec{r}_{ECI}. \tag{3}$$

In the transformation, the polar motion $M(t)$, the Earth's rotation around Z axis $ROT3\big(\theta_{GAST}(t)\big)$ where $\theta_{GAST}(t)$ is the Greenwich apparent sidereal time, the nutation $N(t)$ and the precession $P(t)$ are considered. These matrices are time dependent and the parameters to calculate these matrices are provided by the International Earth Rotation Service (IERS) as an Earth Orientation Parameters (EOP) data [Kelso, 2019].

Atmospheric Drag

The space environment can be considered as vacuum relative to Earth's surface however still some gases exist in atomic or molecular form at an altitude of LEO satellites. Those gases create drag and it is resulted with a secular change in the orbit. Therefore the effect of atmospheric drag on the motion of the satellite can be major in long term propagation. The perturbing acceleration due to atmospheric drag is given as

$$\vec{p}_{Drag} = -\frac{1}{2}\rho v_{rel}\left(\frac{C_dA}{m}\right)\vec{v}_{rel}, \tag{4}$$

Where ρ is density of the gases, $\vec{v}_{rel}$ is the velocity of the satellite with respect to atmosphere, C_d is the drag coefficient, A is the drag area and m is the mass of the satellite. In the calculation of the atmospheric drag, density is an important parameter due to its highly variable feature. Three different atmospheric models which are NRLMSISE-00, MSIS-86 and JACCHIA-70 are used to calculate the density. Only the NRLMSISE-00 is verified with the NASA model website [Papitashvili, 2019]. All three models are time-dependent and take into account solar flux, geomagnetic index, longitude and latitude of the satellite. Solar flux and geomagnetic index can be obtained from the space weather data [Kelso, 2019].

In the software application, inputs are different for the SGP4 and the numerical propagators. For the numerical propagator, physical parameters of the satellite such as mass, drag coefficient and drag area are input initially. Then, epoch is input in Gregorian calendar format and in Universal Coordinated Time (UTC). Afterwards, checkbox for the EOP file is checked and initial state vector is input in ECI frame or ECEF as a user choice, in addition to that, initial state can be input as orbital elements. The conversion between state vector to orbital elements or vice versa can also be provided. In the orbit propagator section, numerical propagator is chosen and timestep of the integrator and duration of the propagation are also input. Duration of the propagation can be input also in terms of orbital period. Afterwards, force models are chosen as J2 or atmospheric drag or both. If the atmospheric drag is chosen as a force model, atmosphere models and parameters panel should be filled. In this panel, firstly the atmosphere model is chosen through the three models. Then, model parameters are chosen as user input or from the space weather data.

For the SGP4 propagator, less input is required compared to numerical propagator. Firstly, checkbox for the EOP file is checked. Then, SGP4 is chosen as orbit propagator and duration of the propagation is input directly or in terms of orbital period. Finally, in order to load TLE data, checkbox for the TLE is checked. The graphical user interface (GUI) of the inputs for the numerical and analytical propagators are shown in Figure 1 and 2.

Figure 1: Inputs of the numerical propagator.

Figure 2: Inputs of the SGP4 propagator.

Groundtrack

The groundtracks provide information about the orbit characteristics of a satellite such as orbital period, orbit type: elliptical or circular, inclination, altitude as well as the coverage. The groundtrack of a satellite can be drawn based on the longitude and latitude values calculated through the orbit propagation. The longitude λ and the geodetic latitude ϕ_{gc}

are calculated from the X, Y, Z components of the position vector of the satellite in ECEF as described in Equations 5 and 6

$$\lambda = \tan^{-1}\left(\frac{Y}{X}\right),\tag{5}$$

$$\phi_{gc} = \sin^{-1}\left(\frac{Z}{\sqrt{X^2 + Y^2 + Z^2}}\right),\tag{6}$$

Eclipse Durations

Eclipse durations are important for the calculation of total power generation and thermal control subsystem design. In the eclipses, power is provided to satellite from the energy stored in batteries which are charged by the solar panels during the sunlit intervals. In the calculation of total power generation, the required energy to charge batteries, and eclipse durations are considered. Also, the satellite is exposed to worst cold condition during the eclipses which is considered in thermal control. In order to keep the temperatures within the satellite in appropriate levels, thermal control subsystem is designed by considering the eclipse durations.

In this study, cylindrical shadow model is used therefore umbra and penumbra conditions are not considered. To determine whether the satellite is in the eclipse or not, the following calculations are done [Curtis, 2013]:

$$\theta = \cos^{-1}\left(\frac{\vec{r}_{sat}}{||\vec{r}_{sat}||} \cdot \frac{\vec{r}_{sun}}{||\vec{r}_{sun}||}\right), \tag{7}$$

$$\boldsymbol{\theta_1} = \cos^{-1}\left(\frac{\boldsymbol{R_e}}{||\vec{\boldsymbol{r}}_{sat}||}\right), \qquad \boldsymbol{\theta_2} = \cos^{-1}\left(\frac{\boldsymbol{R_e}}{||\vec{\boldsymbol{r}}_{sun}||}\right). \tag{8}$$

Here, $\vec{r}_{sat}$ and $\vec{r}_{sun}$ are the position vectors of the satellite and sun, respectively. If $\boldsymbol{\theta_1 + \theta_2} \leq \boldsymbol{\theta}$, then the satellite is in the eclipse.

Solar and Albedo Fluxes

The solar and albedo fluxes are important for the thermal control and power generation. In the calculation of the solar flux on the satellite panels, firstly the solar flux $\boldsymbol{S}$

$$S = \frac{L}{4\pi R^2}, \tag{9}$$

is calculated as a function of distance from the Sun $\boldsymbol{R}$. Here, $\boldsymbol{L}$ is the total radiative power of the Sun in $\boldsymbol{Watt}$. In order to define direction of the satellite panels, RSW (Radial, Along-track, Cross-track) frame is used [Vallado, 2013] with the assumption of a nadir pointing satellite. The unit vectors of the three axis are given as:

$$\hat{R} = \frac{\vec{r}_{sat,ECI}}{||\vec{r}_{sat,ECI}||}, \qquad \widehat{W} = \frac{\vec{r}_{sat,ECI} \times \vec{v}_{sat,ECI}}{||\vec{r}_{sat,ECI} \times \vec{v}_{sat,ECI}||}, \qquad \hat{S} = \widehat{W} \times \hat{R}. \tag{10}$$

Then, direction of the panels are defined in RSW frame as:

$$\hat{p}_R = [1 \quad 0 \quad 0]^T, \quad \hat{p}_{-R} = [-1 \quad 0 \quad 0]^T, \tag{11a}$$

$$\hat{p}_S = [0 \quad 1 \quad 0]^T, \quad \hat{p}_{-S} = [0 \quad -1 \quad 0]^T, \tag{11b}$$

$$\hat{p}_W = [0 \quad 0 \quad 1]^T, \quad \hat{p}_{-W} = [0 \quad 0 \quad -1]^T. \tag{11c}$$

Here, $\boldsymbol{\hat{p}_R}$ and $\boldsymbol{\hat{p}_W}$ represent panels in radial and along-track direction, respectively. In addition, $\boldsymbol{\hat{p}_S}$ corresponds to panel in velocity direction for the circular orbits. Lastly, $\boldsymbol{\hat{p}_W}$ represents panel which is perpendicular to the orbital plane. Negative ones correspond the opposite directions. Then, position vector of the Sun relative to satellite is calculated as

$$\vec{r}_{sun-sat,ECI} = \vec{r}_{sun,ECI} - \vec{r}_{sat,ECI}, \tag{12}$$

in ECI frame. In order to find angle between $\vec{\boldsymbol{r}}_{sun-sat,ECI}$ and panel normals given in (11), $\vec{\boldsymbol{r}}_{sun-sat,ECI}$ has to be defined in RSW frame. So, the transformation between ECI to RSW is required. The transformation matrix is given as:

$$M_{ECI \rightarrow RSW} = \begin{bmatrix} R_x & R_y & R_z \\ S_x & S_y & S_z \\ W_x & W_y & W_z \end{bmatrix}. \tag{13}$$

Then, $\vec{\boldsymbol{r}}_{sun-sat,ECI}$ is written in RSW frame as

$$\vec{r}_{sun-sat,RSW} = M_{ECI \rightarrow RSW}\vec{r}_{sun-sat,ECI}, \tag{14}$$

by using the transformation matrix $\boldsymbol{M_{ECI \rightarrow RSW}}$.

Finally, the amount of solar flux falling on each panel is calculated as follows:

$$\Phi_R = \cos^{-1}\left(\frac{\vec{r}_{sun-sat,RSW}}{||\vec{r}_{sun-sat,RSW}||} \cdot \hat{p}_R\right) \times S, \quad \Phi_R = \cos^{-1}\left(\frac{\vec{r}_{sun-sat,RSW}}{||\vec{r}_{sun-sat,RSW}||} \cdot \hat{p}_{-R}\right) \times S, \tag{15a}$$

$$\Phi_S = \cos^{-1}\left(\frac{\vec{r}_{sun-sat,RSW}}{||\vec{r}_{sun-sat,RSW}||} \cdot \hat{p}_S\right) \times S, \quad \Phi_S = \cos^{-1}\left(\frac{\vec{r}_{sun-sat,RSW}}{||\vec{r}_{sun-sat,RSW}||} \cdot \hat{p}_{-S}\right) \times S, \tag{15b}$$

$$\Phi_W = \cos^{-1}\left(\frac{\vec{r}_{sun-sat,RSW}}{||\vec{r}_{sun-sat,RSW}||} \cdot \hat{p}_W\right) \times S, \quad \Phi_W = \cos^{-1}\left(\frac{\vec{r}_{sun-sat,RSW}}{||\vec{r}_{sun-sat,RSW}||} \cdot \hat{p}_{-W}\right) \times S. \quad (15c)$$

Here, cosines are the angles between direction of the sun and panel normals, also S is the solar flux given in (9).

Albedo is another heat source for the LEO missions. It is defined as the reflected Sun light from the Earth and depends on the reflectivity of the surface. In this work, a simplified version of an albedo model developed by [Bhanderi, 2019] is used to calculate the albedo flux on a given satellite.

Communication Intervals

Communication intervals are important for the times of data transfer between satellite and ground station. In order to determine communication intervals, elevation angle of the satellite relative to the ground station is calculated. In addition, azimuth angle is also required for the satellite tracking. Those two angles are calculated as follows:

$$\vec{\rho}_{ECEF} = \vec{r}_{sat,ECEF} - \vec{r}_{site,ECEF}. \quad (16)$$

where $\vec{\rho}_{ECEF}$ is the position vector of the satellite relative to ground station in ECEF. To obtain azimuth and elevation angles, South-East-Zenith (SEZ) coordinate system is used [Vallado, 2013]. Then, the transformation between ECEF to SEZ is given as:

$$\vec{\rho}_{SEZ} = ROT2(90° - \phi_{gc})ROT3(\lambda)\vec{\rho}_{ECEF}. \quad (17)$$

Here, $ROT2$ and $ROT3$ are the rotation around Y and Z axis, respectively. Also, λ and ϕ_{gc} are the longitude and geodetic latitude of the ground station. Finally, the elevation angle el and the azimuth angle β are calculated as

$$el = \sin^{-1}\left(\frac{\rho_{SEZ,Z}}{||\vec{\rho}_{SEZ}||}\right), \quad (18)$$

$$\beta = \sin^{-1}\left(\frac{\rho_{SEZ,E}}{\sqrt{\rho_{SEZ,S}^2 + \rho_{SEZ,E}^2}}\right), \quad (19)$$

where $\rho_{SEZ,S}$, $\rho_{SEZ,E}$, $\rho_{SEZ,Z}$ are the components of $\vec{\rho}_{SEZ}$. Also, the quadrant ambiguity is considered for the azimuth angle β.

In the software, location of the ground station is input as longitude, latitude and altitude. Also, a limit elevation angle is specified for the start and finish times of the communication. If the satellite is over the elevation limit, ground station can communicate with the satellite.

Figure 3: Inputs for the communication intervals.

Imaging Opportunities

Imaging oppurtunities are important for capturing the image at the time that satellite passes over the target. In order to determine conditions for the imaging opportunities, firstly the position vector of the target relative to the satellite is calculated as

$$\vec{r}_{rel,ECI} = \vec{r}_{target,ECI} - \vec{r}_{sat,ECI}, \qquad (20)$$

in ECI frame. Then, transformation from ECI frame to RSW frame is applied:

$$\vec{r}_{rel,RSW} = M_{ECI \to RSW}\vec{r}_{rel,ECI}. \qquad (21)$$

To find time that satellite passes over the target, unit vector in nadir direction is written as

$$\hat{r}_{nadir,RSW} = \begin{bmatrix} -1 & 0 & 0 \end{bmatrix}^T, \qquad (22)$$

in RSW frame. Afterwards, angle between $\vec{r}_{rel,RSW}$ and $\hat{r}_{nadir,RSW}$ is calculated as:

$$\vartheta = \cos^{-1}\left(\frac{\vec{r}_{rel,RSW}}{||\vec{r}_{rel,RSW}||} \cdot \hat{r}_{nadir,RSW} \right). \qquad (23)$$

There are two possibilities of $\vartheta = 0°$; the satellite is just over the target or the nadir direction of the satellite makes an angle of $180°$ with the target. In order to eliminate the second possibility, elevation angle of the satellite is also calculated. Actually the time that satellite passes just over the target corresponds to time that elevation angle is $90°$.

In the software, location of the imaging target is input as longitude, latitude and altitude. Also, a limit camera angle is specified for the start and finish times of the imaging. If the elevation angle of the satellite is positive, in other words if the satellite is above the horizon relative to target, and also if ϑ is below the limit camera angle, then a possibility of capturinf the image of the target can be found.

Figure 4: Inputs for the imaging opportunities.

Satellite Modes

The satellite has different operational modes. Each mode includes different power consumption, data generation and attitude profile. In this study, nominal mode, communication mode, imaging mode and safe mode are considered. With respect to these modes, power consumption and data generation profiles are computed.

In the software, mode plan is loaded by checking the relevant checkbox. Currently, modes are input from the text file. The format of the text file is described in Figure 5. Modes are executed according to user defined start and finish times. In addition, one mode can be used in several times with different start and finish times. The values of power consumption and data generation of the corresponding modes are input by the user.

Figure 5: Satellite modes description.

RESULTS

In this section, outputs of the software are presented and compared with General Mission Analysis Tool (GMAT).

Figure 6: Outputs of the software.

The software is developed in MATLAB environment. For the NRLMSISE-00, MSIS-86 and JACCHIA-70 atmosphere models, the MATLAB codes in [Mahooti, 2015], [Mahooti, 2017b], [Eagle, 2013] are modified, respectively. For the albedo model, the MATLAB code in [Bhanderi, 2009] is modified. Lastly, for the calculation of ECI to ECEF transformation matrix and position vector of sun, the MATLAB code in [Mahooti, 2017b] and [Mahooti, 2016] are modified, respectively. Also, EOP and space weather files are taken from the Celestrak website [Kelso, 2019].

Orbit Propagation: In the software, both numerical integration and SGP4 model are utilized for the orbit propagation. The inputs used to obtain results of the numerical orbit propagation are given in Figure 7. In the left-hand side, physical parameters of the satellite, initial epoch and initial state vector are entered. In the right-hand side, firstly step size of the numerical integration and duration of the propagation are entered. Then, force models are chosen as J2 and atmospheric drag. Finally, the atmosphere model and its parameters are specified. The results are obtained as state vector in two different coordinate systems and compared with GMAT.

Figure 7: Inputs for the numerical orbit propagation.

Initial time	01.07.2015 / 13:09:58 (UTC)					
Final time	02.07.2015 / 13:09:58 (UTC)					
	State vector in ECI frame					
	X (km)	Y (km)	Z (km)	VX (km/s)	VY (km/s)	VZ (km/s)
Software	-1297.320	-6637.019	-1254.530	-1.244	-1.161	7.420
GMAT	-1297.356	-6637.051	-1254.313	-1.244	-1.161	7.420

Table 1: Comparison of the state vector in ECI frame for one-day numerical propagation.

Initial time	01.07.2015 / 13:09:58 (UTC)					
Final time	02.07.2015 / 13:09:58 (UTC)					
	State vector in ECEF					
	X (km)	Y (km)	Z (km)	VX (km/s)	VY (km/s)	VZ (km/s)
Software	-5285.128	4218.583	-1256.141	-0.141	2.035	7.418
GMAT	-5285.139	4218.630	-1255.923	-0.141	2.035	7.418

Table 2: Comparison of the state vector in ECEF for one-day numerical propagation.

It is observed that the maximum positional difference is approximately 200 meters at the end of one-day propagation. The most possible reason of this difference is due to the models used in the calculation of the atmospheric drag. In GMAT, MSISE90 is used as atmospheric model however in the developed software, NRLMSISE-00 model is used., Therefore, the acceleration

due to atmospheric drag is calculated differently for each software and this is observed in the positional difference.

Groundtrack: The groundtrack is drawn based on the longitude and latitude of the satellite during the orbit propagation.
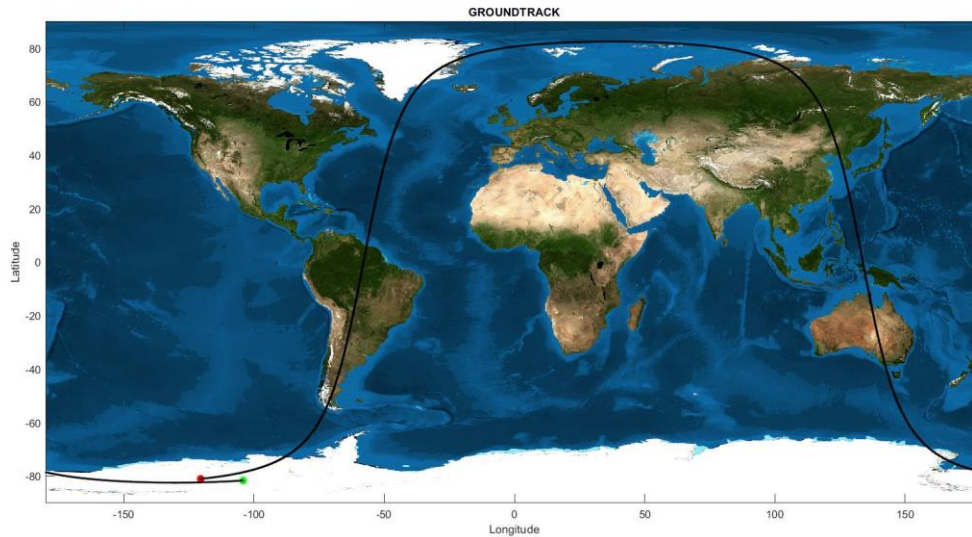

Figure 8: The groundtrack for one period. Green and red dots represent the initial and final position of the satellite, respectively.

Eclipse Durations: The results of the eclipse durations are given as start and finish time of the eclipse and compared with GMAT. GMAT uses penumbra and umbra conditions but they are not considered in the developed software. Therefore, it is assumed that satellite is in the eclipse at penumbra in the comparison with GMAT. The results of the first and the last eclipses are presented for one-day propagation.

	Start Time (UTC)	Finish Time (UTC)
Software	01.07.2015 / 14:44:21	01.07.2015 / 15:19:30
GMAT	01.07.2015 / 14:44:23	01.07.2015 / 15:19:29

Table 3: Comparison of the eclipse times for the first eclipse in one-day propagation.

	Start Time (UTC)	Finish Time (UTC)
Software	02.07.2015 / 11:13:27	02.07.2015 / 11:48:35
GMAT	02.07.2015 / 11:13:29	02.07.2015 / 11:48:35

Table 4: Comparison of the eclipse times for the last eclipse in one-day propagation.

It is seen that the maximum time difference is around 2 seconds. The most likely reason of the difference is the assumption in calculation of eclipses. In the software, cylindrical eclipse model is used instead of conic model which GMAT uses.

Solar Flux: The solar flux falling on the satellite panels are plotted during one orbit. The nadir pointing is used as attitude profile. Results are compared with the software of TUBITAK UZAY's mission analysis software.
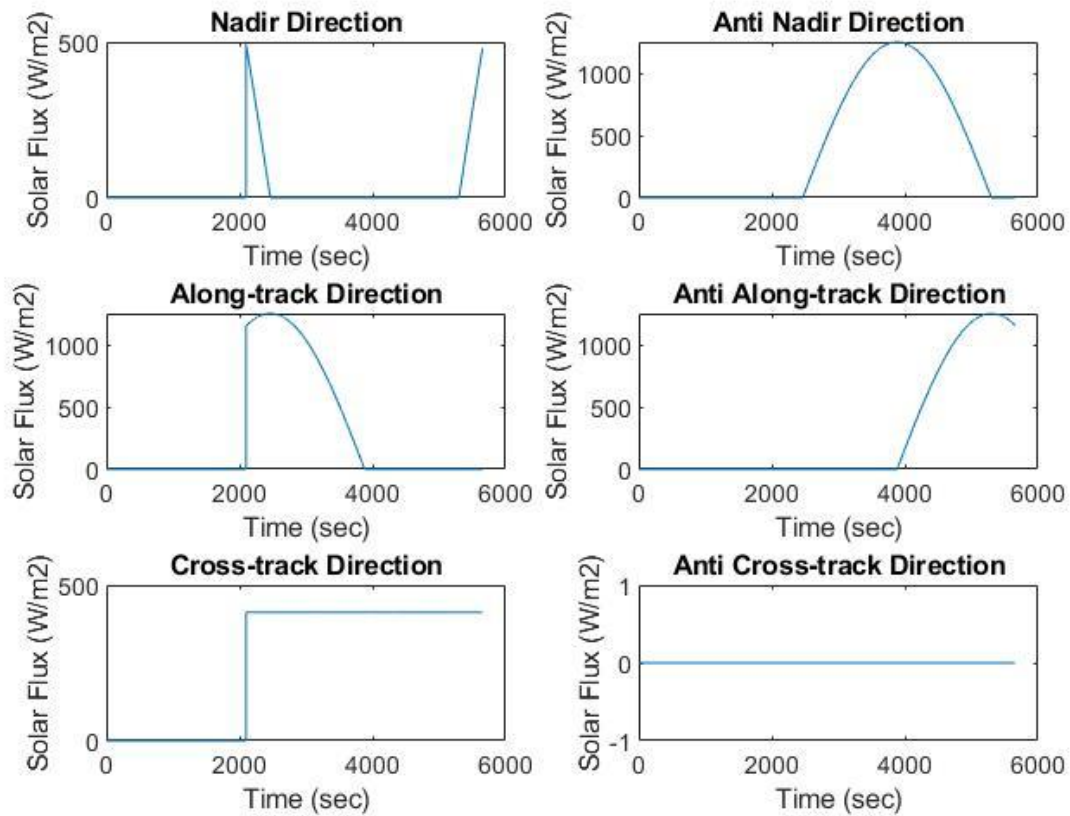
Figure 9: The solar flux profiles obtained from the software for each panel during one orbit.

The comments of the Figure 9 are provided by considering the orbit given in Figure 7. It is seen that at the beginning, there is no solar flux falling on the panels due to the eclipse. When the satellite starts to exit from the eclipse, most of the solar flux falls on the panel in along-track direction. Actually, it is reasonable because just after the eclipse, the first panel which sees the Sun in a wide angle is in along-track direction. Conversely, when the satellite starts to enter the eclipse, the last panel which sees the Sun in a wide angle is in negative along-track direction. This is the reason of increase in the solar flux in negative along-track direction while the satellite is entering the eclipse. In addition to the along-track direction, solar flux profiles in nadir and negative nadir directions are also reasonable. Panel in nadir direction sees the Sun slightly only when the satellite enters or exits the eclipse. Also, the time that panel in along-track direction gets out of the sunlit, nearly at 4000 second, corresponds to time that maximum solar flux falling on panel in negative nadir direction. Lastly, the solar flux profiles in cross-track and negative cross-track directions depend on orientation of the orbital plane. Since the orbit is Sun-synchronous, solar flux profiles are constant.
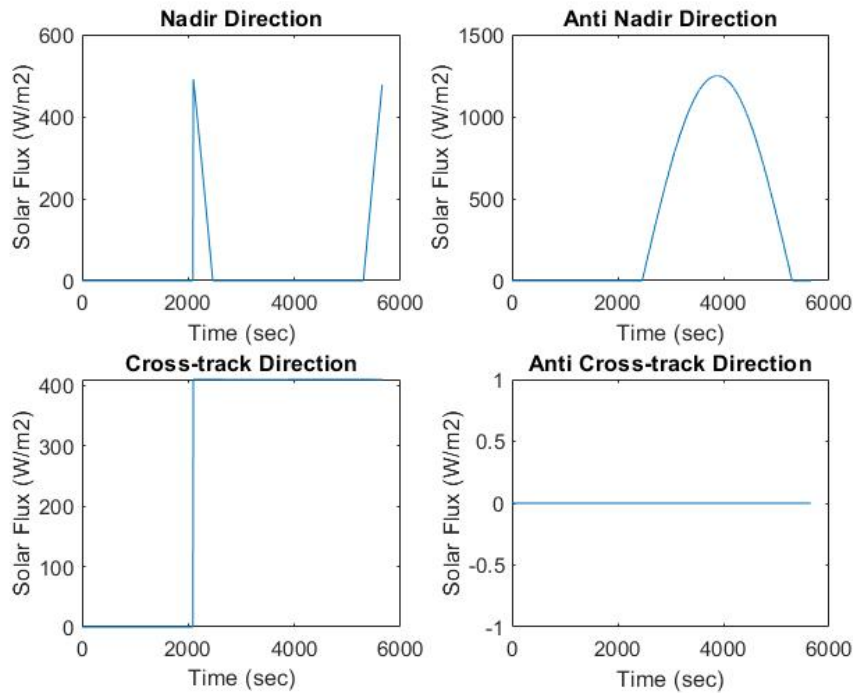
Figure 10: The solar flux profiles obtained from the TUBITAK UZAY software during one orbit.

The solar flux profiles are verified with the TUBITAK UZAY's mission analysis software.

Albedo Flux: The albedo flux falling on the satellite panels are plotted during one orbit. Since the nadir pointing is used as attitude profile, it is assumed that all the albedo radiation falls on panel in nadir direction.
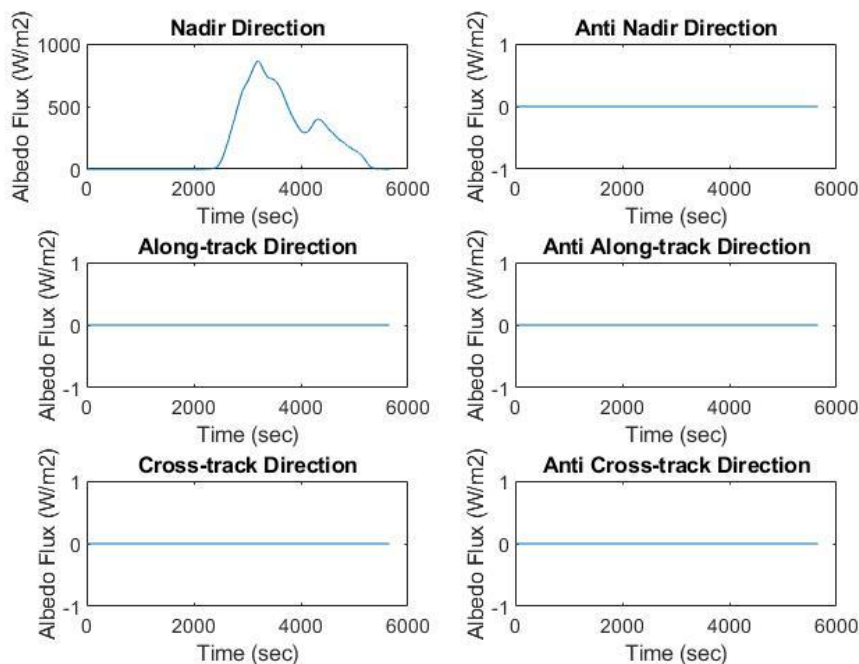

Figure 11: The albedo flux profiles obtained from the software for each panel during one orbit.

It is seen that at the beginning, there is no albedo flux falling on the panels due to the eclipse. When the satellite starts to exit from the eclipse, albedo flux also starts to increase because the satellite starts to pass over the areas on Earth where it is exposed to more sunlight. The profile makes peak at the time when the satellite passes over the area where it is exposed to the maximum sunlight. After that, it makes another peak which is smaller than the previous one. This peak occurs as the satellite passes over an area that have high reflectivity. Then, the albedo flux decreases until the eclipse as expected.

Communication Intervals: The results of the communication intervals are given as start and finish times of the communication and compared with GMAT. The location of the ground station is chosen as Ankara. Also, a limit elevation is entered in order to determine start and finish times of the communication. During one-day propagation, two contacts happen with the ground station. Those are given in Tables 5 and 6.

Figure 12: The location of the ground station and limit elevation.

	Start Time (UTC)	Finish Time (UTC)
Software	01.07.2015 / 19:59:22	01.07.2015 / 20:06:42
GMAT	01.07.2015 / 19:59:21	01.07.2015 / 20:06:43

Table 5: Comparison of the communication times for the first contact in one-day propagation.

	Start Time (UTC)	Finish Time (UTC)
Software	02.07.2015 / 09:02:20	02.07.2015 / 09:09:21
GMAT	02.07.2015 / 09:02:19	02.07.2015 / 09:09:21

Table 6: Comparison of the communication times for the last contact in one-day propagation.

Imaging Opportunities: The results of the imaging opportunities are given as start and finish times of the imaging according to the camera limit angle. The camera angle is the angle between nadir and target direction. When it is zero, it means that satellite passes just over the target. The limit of the camera angle determines the start and finish times of the imaging. In addition to those, time that satellite passes just over the target can be seen from the results. This also corresponds to time that elevation angle is $90°$. Since GMAT has not any function for the imaging opportunities, results are not directly compared with GMAT. For the comparison, firstly the longitudes and latitudes of the satellite are obtained during one-day propagation in GMAT. Then, arbitrary longitude and latitude are chosen as target location among those values and input to the software as shown in Figure 13. The results obtained from the software are presented in Table 7 as camera angle, elevation angle and time that satellite passes just over the target. Also, the results of GMAT are presented in Table 8 as the time that satellite passes just over the chosen longitude and latitude, namely target location.

Figure 13: Location of the target and limit angle.

	Time that satellite passes just over the target.		
	Time (UTC)	Camera Angle (deg)	Elevation (deg)
Software	01.07.2015/16:19:20	0.0480	89.9991

Table 7: Results obtained from the software for time that satellite passes just over the target.

	Time that satellite passes just over the target.		
	Time (UTC)	Longitude (deg)	Latitude (deg)
GMAT	01.07.2015/16:19:20	-158.0314	-82.1047

Table 8: Results obtained from the GMAT for time that satellite passes just over the target.

It is seen that time that satellite passes just over the target is verified with GMAT. Also, from the software, it is obtained that camera angle is almost 0° at that time. It means nadir direction and target direction are coincided, hence, target is in the nadir direction. Beside the camera angle, elevation angle of the satellite is also obtained as almost 90° as expected.

Satellite Modes: In the software, four satellite modes are used. Those are nominal mode, communication mode, imaging mode and safe mode. The mode definitions are done in terms of power consumption and data generation. In addition, start and finish times of each mode are specified for the execution order. Therefore, each mode can be used several times with different start and finish times. The mode definitions and plans are input to the software.

Start Time (s)	Finish Time (s)	Power Consumption (W)	Data Generation (Mb)	Modes
0	5654	4	2	Nominal
5655	11308	4	2	Nominal
11309	16962	4	2	Nominal
16963	22616	5	3	Imaging
22617	28270	4	2	Nominal
28271	33924	4	2	Nominal
33925	39578	8	-4	Communication
39579	45232	4	2	Nominal
45233	50886	4	2	Nominal
50887	56540	4	2	Nominal
56541	62194	5	3	Imaging
62195	67848	4	2	Nominal
67849	73502	8	-4	Communication
73503	79156	4	2	Nominal
79157	84810	3	1	Safe
84811	86400	3	1	Safe

Table 9: The mode plan for one-day propagation.

The results are given in Figure 14 as power and data profiles. It is seen that profiles match with the inputs given in Table 8.
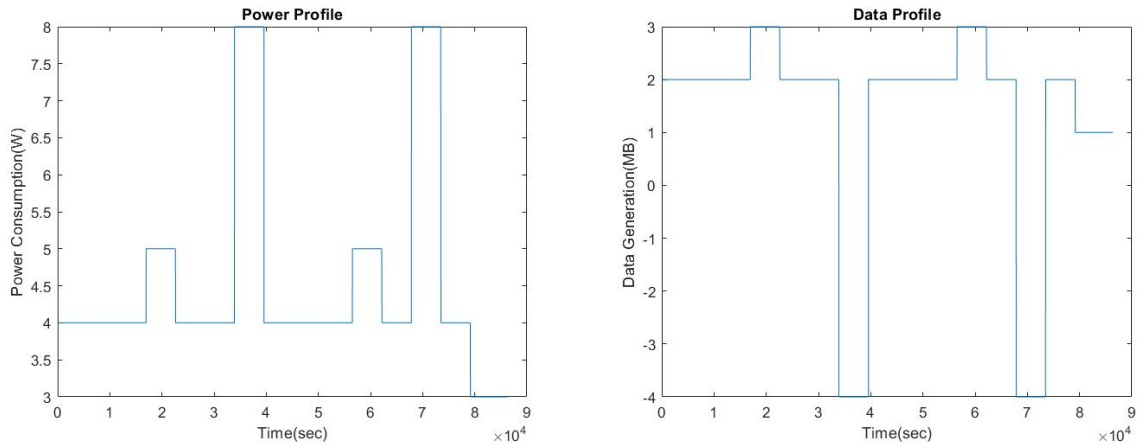

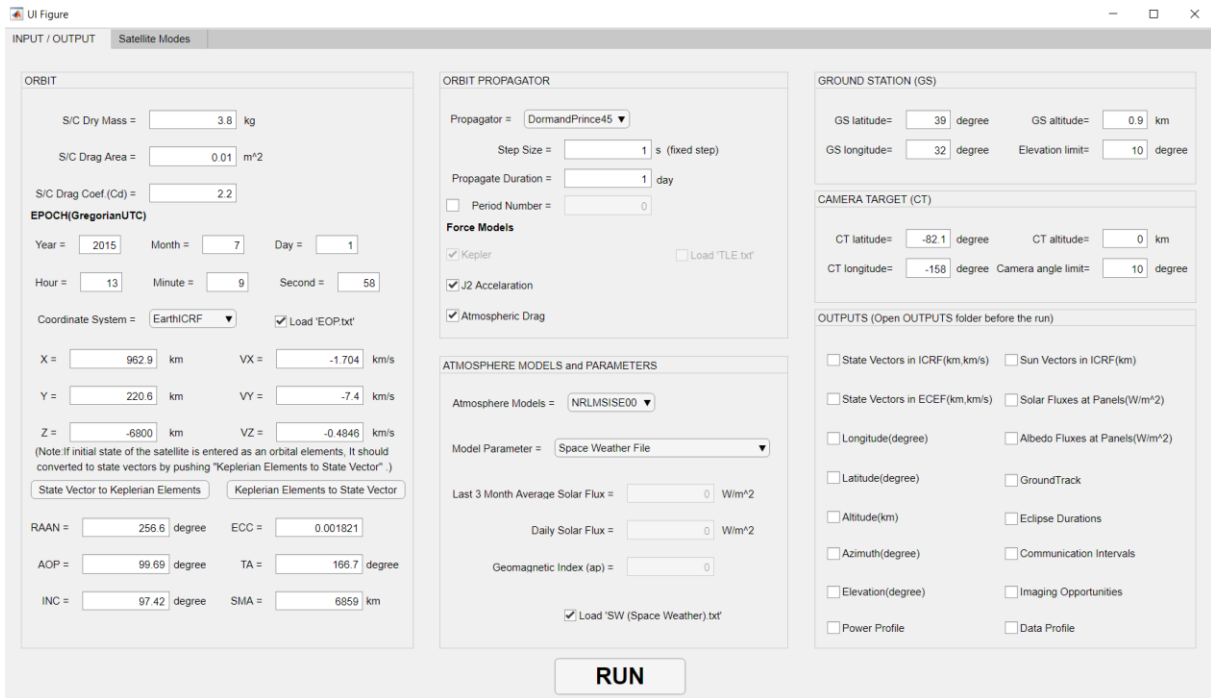Figure 14: Power and data profiles for one-day propagation.

Figure 15: General view of the software.

CONCLUSIONS

In this work, a mission analysis software is developed by university students with a user-friendly GUI in MATLAB environment. The software includes several functions related to LEO missions such as orbit propagation with the options of SGP4 and numerical integration andgroundtrack plots as well as calculation of eclipse durations, solar and albedo fluxes on the satellite panels, communication intervals, imaging opportunities and parameters specific for satellite modes. The results of the most functions are compared and verified with GMAT. For the further analysis, it is considered to include attitude profiles for each mode, and thermal analysis capabilities. At the end of this work, it is aimed that to develop a highly capable mission analysis software which can be used for the design, analysis and operations of LEO small satellites.

ACKNOWLEDGEMENTS

References

Bhanderi, D. (2006). Modeling Earth Albedo Currents on Sun Sensors for Improved Vector Observation. AIAA Guidance, Navigation, and Control Conference and Exhibit. doi:10.2514/6.2006-6592

Bhanderi, D. D. V. (2009) *Mathworks: Earth Albedo Toolbox*. https://www.mathworks.com/matlabcentral/fileexchange/11226-earth-albedo-toolbox

Curtis, H. D. (2013) *Orbital Mechanics for Engineering Students*, 3. Edition, Elsevier.

Dormand, J. R. , Prince, P. J. (1980) *A family of embedded Runge-Kutta formulae*, Journal of Computational and Applied Mathematics, Vol. 6.

Eagle, D. (2013) *Mathworks: A Matlab Implementation of the Jacchia Atmosphere Model*. https://www.mathworks.com/matlabcentral/fileexchange/41752-a-matlab-implementation-of-the-jacchia-atmosphere-model

Fortescue, P. , Stark, J. , Swinerd, G. (2003) *Spacecraft Systems Engineering*, 3. Edition, Wiley.

Gaposchkin, E. M. , Coster, A. J. (1988) *Analysis of Satellite Drag*, The Lincoln Laboratory Journal, Vol. 1.

Garcia, A. L. (2000) *Numerical Methods for Physics*, 2. Edition, Prentice-Hall.

Gilmore, D. G., & Donabedian, M. (2003). Spacecraft thermal control handbook. Reston, VA: American Institute of Aeronautics and Astronautics.

Kelso, T. S. (2019) *EOP and Space Weather Data*. https://celestrak.com/SpaceData/

Kulu, E. (2019) Nanosats Database

https://www.nanosats.eu/

Mahooti, M. (2015) *Mathworks: NRLMSISE-00 Atmosphere Model.*
https://www.mathworks.com/matlabcentral/fileexchange/56253-nrlmsise-00-atmosphere-
model

Mahooti, M. (2016) *Mathworks: Sun Position.*

https://www.mathworks.com/matlabcentral/fileexchange/56042-sun-position

Mahooti, M. (2017a) *Mathworks: ICRS-ITRS transformation.*

https://www.mathworks.com/matlabcentral/fileexchange/61957-icrs-itrs-transformation

Mahooti, M. (2017b) *Mathworks: MSIS-86 Atmosphere Model.*

https://www.mathworks.com/matlabcentral/fileexchange/65117-msis-86-atmosphere-
model

Montenbruck, O. , Gill, E. (2000) *Satellite Orbits-Models, Methods and Applications*, 1.
Edition, Springer.

Papitashvili, N. (2019) *Community Coordinated Modeling Center: NRLMSISE-00
Atmosphere Model.*

https://ccmc.gsfc.nasa.gov/modelweb/models/nrlmsise00.php

Vallado, D. A. (2013) *Fundamentals of Astrodynamics and Applications*, 4. Edition,
Microcosm Press.

Yağlıoğlu, B., Ataş, Ö., Kahraman, D., Köse, S., Tekinalp, O., Süer, M.,(2019) "A Multi-
National Multi-Institutional Education Framework: APSCO SSS-2B CubeSat Project ",
IEEE Xplore/RAST 2019, Istanbul, Türkiye, 11-14 June 2019.